ISSN: 2454-9940

INTERNATIONAL JOURNAL OF APPLIED SCIENCE ENGINEERING AND MANAGEMENT

E-Mail :
editor.ijasem@gmail.com
editor@ijasem.org

www.ijasem.org

INTERNATIONAL JOURNAL OF APPLIED SCIENCE ENGINEERING AND MANAGEMENT

ISSN2454-9940
www.ijsem.org
Vol 8 Issue 3 July 2014

HYPERSPECTRAL REMOTE SENSING AND GIS USES IN EVALUATING AIR POLLUTION AND FOREST HEALTH

Dr. Z. Abdul Rahim

ABSTRACT

This study aims to assess the impact of air pollution on conifer tree health in two different regions: the Pyrenees in Catalonia, Spain, and the Sierra Nevada in California, USA. To achieve this, we will use GIS analysis to look at how different pressures vary along natural gradients in topography and how forest health indices from remote sensing measure up. However, P. uncinata in Spain was first measured using the Ozone Injury Index (OII), which was originally developed for P. ponderosa and P. jeffreyi in the country. The OII field measure were supplemented with criteria such as chlorotic mottling, needle retention, needle length, and crown depth. The target bioindicator species achieved a total accuracy of close to 80% in species-level classifications using AVIRIS and CASI hyperspectral imaging. The R2 values for Catalonia and California, which were 0.68 and 0.56, respectively, with a p-value less than 0.0001, were greatly enhanced by integrating remote sensing indices with geographic information system characteristics that pertain to microsite ozone uptake variability. In Catalonia, the integrated OII, which incorporated the remote sensing index PRI and an ambient ozone three-year average, outperformed the multiple regression models.

Keywords: hyperspectral remote sensing, airpollution, ozone, forest health, GIS

INTRODUCTION

A major obstacle in the bio-monitoring of air pollution impacts on forest health is scaling up from laboratory experiments and plot studies to landscape-scale investigations, where natural gradients in environmental condition can alter plant uptake of ambient pollution levels [8], [9]. Observational studies of bioindicator species in Mediterranean climates have shown that there can be a large seasonal disconnect between ambient ozone concentrations and ozone uptake [7], [8], [9]. Using GIS to estimate tree physiological status [1], [4] in combination with observational studies field studies of ozone injury takes advantage of natural gradients which affect ozone uptake to integrate environmental condition with physiological measures of ozone injury ([10]). GIS variables can estimate environmental factors indirectly related to plant water usage (elevation, aspect, and solar irradiance) and availability (distance to water sources, slope, topographic curvature, and topographic convergence). By including proxies

Associate Professor, Department of Civil Engineering,
Maulana Azad National Urdu University, Hyderabad
Email id: dr.zabdulrahim@gmail.com

related to both plant water usage and availability, an improved approximation of ozone stomatal conductance is obtainedvia GIS variables alone. Remote sensing of plant physiological condition ([12]) then allows for theextrapolation of these field studies and GIS analyses to full landscape scale analyses across large environmental gradients ([11]). Here, the capacity for species level classification mapping of bioindicator species is veryimportant for the subsequent interpretation of the physiological health variability assessment of that bioindicator across environmental gradients.

Specifically, the Advanced Visible Infrared Imaging Spectrometer (AVIRIS: 224 spectral bands from 400-2500 nm) of the Jet Propulsion Laboratory of the National Aeronautics and Space Administration (NASA) in the USA and the Compact Airborne Spectrographic Imager (CASI: 72 spectral bands from 430-950nm)) of the Cartographic Institute of Catalonia in Spain, provide sufficiently detailed spectral and spatial (<4 m) information to map the location and physiological conditions of specific plant species [9], [11]; [12]). In this paper, we present two case studies of the combination of hyperspectral remote sensing with GIS and its potential for landscape scale analyses of bioindicator species ecological status and risk assessments of ozone impacts on forest health. Improvements in the remote sensing of plant health are also investigated using GIS models as proxies of ozone uptake in order to bring ambient ozone mixing ratio measurements into an ecological context at the landscape scale.

I. METHODS

A. Passive Monitoring of Air Pollution

In YOSE and SEKI passive ozone monitoring data wasdownloaded through a national passive sensor monitoring program maintained by the US National Park Service (NPS). For more details see [5] or: (http://www.nature. nps.gov/air/studies/passives.cfm#procedures).

In Spain, the air pollution passive monitoring sampling included ozone, NOx, and VOCs ambient concentrationsmonitoring at ten stations along altitudinal gradients (1100m to 2300m) of the Meranges and Guills transects, conducted by the CREAF lab at the Autonomous University of Barcelona. For further details on the data collection and analysis procedures see [2] and [6].

ISSN2454-9940
www.ijsem.org
Vol 8 Issue 3 July 2014

B. Field Assessments of Ozone Injury

As a biomonitoring visual assessment of ozone-induced foliar injury which represents over 20 years of ozone biomonitoring research development [3], the Ozone Injury Index (OII) is expected to be similarly useful in application the ozone-sensitive species of other regions such as the Pyrenees Mountains of Spain. The only adjustment made tothe OII protocol in its adaptation to *P. uncinata* in Catalonia was in the needle length (LGT) component, to provide a reference to a baseline "average healthy needle" for the *P. uncinata,* calculated as 6cm.

Needle whorl samples were collected along 10 transects in YOSE and SEKI valleys in California with 100 m transect spacing and 50 meter tree spacing. Samplingheight was limited to 10 m due to sampling pole length, limiting data collection as foliage is often not present in the lower part of the canopy in 40m+ tall older specimens of these species. In Catalonia, a total of five trees were sampled in a perpendicular transect at each of the nine air pollution sampling sites and spaced a minimum of 10 metersapart.

C. GIS Models Relevant to Ozone Uptake and Impacts

Spatially-explicit GIS layers were used to place small study plots in their context at the landscape scale and help elucidate the variability of drought stress and ozone stomatal uptake across the landscape [8], [9]; [10]). GIS analyses were developed based on digital elevation models at a 10 meter resolution, including inverse distance weighting from water sources, slope, aspect, the Topographic Convergence Index [1], and incident solar irradiation [4]. All of these GISlayers were developed using ArcGIS (ESRI 2011) with digital elevations maps from the ASTER GDEM dataset, a product of METI and NASA.

D. Hyperspectral Image Acquisition, Calibration, and Analyses

NASA was contracted to collect AVIRIS (Airborne Visible Infrared Imaging Spectrometer) imagery, measuring 224 contiguous narrow spectral bands from 400 to 2500 nanometers. Imagery was collected in high resolution mode(~ 4 m) over YOSE and SEKI central valleys on October 2, 2002. Spectral reflectance calibration targets were measuredat the time of overflight using an ASD Field Spec Pro (Analytical Spectral Devices Denver, CO, USA) portable full spectral range spectrophotometer. Atmospheric and secondary spectral calibration was applied to the image using the atmospheric correction program ACORN, basedon the ModTran-4

radiative transfer code developed by the US Air Force, (Atmospheric CORrection NOW, IMSpec ILL, Palmdale, CA) using Mode 1.5, followed by and empirical line improved calibration using field spectra.

Through the Cartographic Institute of Catalonia, CASI (Compact Airborne Spectral Imager, 72 bands from 400 nm to 900 nm, 3 meter spatial resolution) data was collected covering 2km wide swaths over two transects in the Catalan Pyrenees in May of 2007. Field spectral targets were measured using a UNISPEC (PP Systems) during over flight for applying a similar hybrid atmospheric correction and conversion to surface reflectance values, and empirical line calibration technique using the FLAASH software plug-in for ENVI, which is also based on a modified version of the ModTran-4 algorithm.

The next step in imagery analysis required identifying the location (pixels) dominated by the bioindicator species. The following steps were applied to simplify, reduce excess noise for the purposes of image classification. The first step was to apply a high NDVI mask of NDVI > 0.40. On the masked images, a MNF transform was performed, removing image background noise and producing a subset of coherent and uncorrelated MNF bands. For the final classifications, a select optimal subset of the MNF bands and remote sensing vegetation indices directly related to real bio-physical properties were stacked into a single image and processed using the maximum likelihood classification algorithm in ENVI. These classification mapping techniques were then validated using separate training and testing datasets for accuracy assessments. In all image classifications, separate training and testing datasets were used based on a 60:40 data split for the target species.

INTERNATIONAL JOURNAL OF APPLIED SCIENCE ENGINEERING AND MANAGEMENT

ISSN2454-9940
www.ijsem.org
Vol 8 Issue 3 July 2014

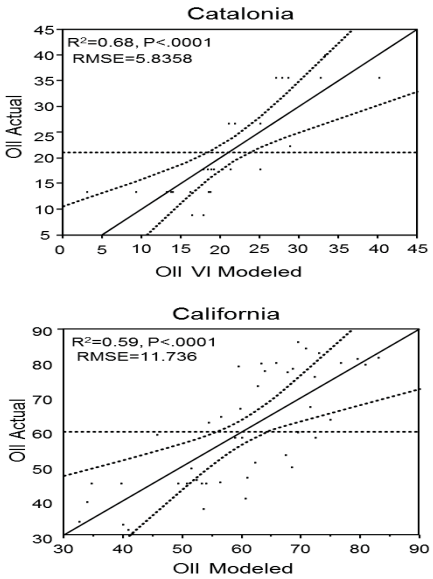

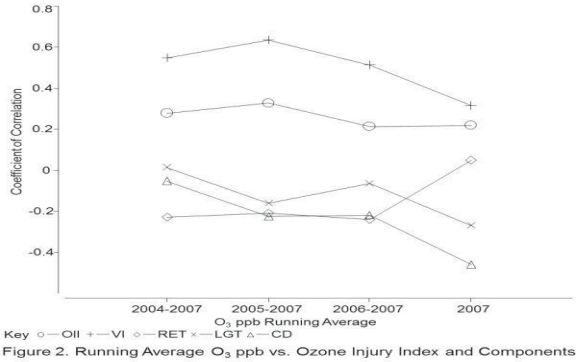

Figure 2. Running Average O_3 ppb vs. Ozone Injury Index and Components

Figure 1. Modeling ozone damage (OII) in Catalonia (top) and California (bottom) using remote sensing vegetationindices and GIS variables. The inclusion of GIS variables improved the significance between ozone injury and remote sensing vegetation indices with the R2 values reaching 0.68 and 0.59 for Catalonia and California, respectively.

II. RESULTS

A. Ozone Monitoring and Injury Assessments

Ozone mixing ratios as measured within the study area in Catalonia ranged from 31 ppb at the valley floor at 1250m altitude to near to 60 ppb at 2300m altitude, with a good relationship between the passive and active sensors: ozone mixing ratio $_{\text{passive sampler}}$ = 0.9468 * mixing ratio $_{\text{monitor}}$ +7.4734, R^2 = 0.73, p < 0.0001 [2]. In California, the average yearly ozone mixing ratios for California in 2002 ranged from 35 ppb to 65 ppb, with a 95% confidence interval between EPA approved active and Ogawa passive sensors at 5ppb according to the NPS survey [5].

The Ozone Injury Index (OII) results values obtainedby the transfer for the OII metrics from ponderosa and Jeffrey's pine tos to the mountain pine in Catalonia were similar and realistic. The average values and standard deviations were 47.2(17.5), 64.4(17.2), and 52.9(16.0) for Catalonia, Yosemite (YOSE) and Sequoia/Kings Canyon(SEKI), respectively. This supports the transfer of the OII to other conifers in similar ecosystems and ambient ozone pollution levels as observed in California. Figure 2. OII and Components Correlation vs. Yearly Running Averages of ambient ozone exposure in Catalonia.

INTERNATIONAL JOURNAL OF APPLIED SCIENCE ENGINEERING AND MANAGEMENT

ISSN2454-9940
www.ijsem.org
Vol 8 Issuse 3 July 2014

B. Imagery Species Classifications

Good classification accuracies were achieved for the bioindicator species from the AVIRIS and CASI imagery. In California, the two species have like sensitivities to O_3 and spectral properties, and as such were combined for the imagery classifications. Classification of ponderosa pine in YOSE used eight classes (the six most common tree species, shadowed vegetation and unclassified pixels) produced 75%accuracy for ponderosa pine. Classification in SEKI also used eight classes (the six most common tree species, shadowed vegetation and unclassified pixels) and produced 82% accuracy for Jeffrey's pine. The species-level classification accuracies of the CASI imagery using nine classes for both scenes (urban, rock, water, pasture, mountain pine, mixed bushes, agriculture, snow, and unclassified pixels) resulted 76 % accuracy for mountain pine for the Meranges flight line and 78% accuracy formountain pine for the Guils flight line.

C. Multiple Regression Analyses of Ozone Injury Assessments, Remote Sensing and GIS

Multiple linear regressions (MLR) were first produced using a combination of remote sensing vegetation indices and GIS variables for both Catalonia and California. Then, further improvements were pursued using remote sensing with ambient ozone pollution for the Catalonia site only, as there was more extensive coverage of air pollution and variability between sites in Catalonia. Combining multiple remote sensing indices, GIS variables, and multiple year ambient ozone measurements for Catalonia produced the highest R^2 value of 0.77, and a more parsimonious R^2 of 0.56 with onlythe PRI index and a three-year average of ambient ozone.

INTERNATIONAL JOURNAL OF APPLIED SCIENCE ENGINEERING AND MANAGEMENT

ISSN2454-9940
www.ijsem.org
Vol 8 Issue 3 July 2014

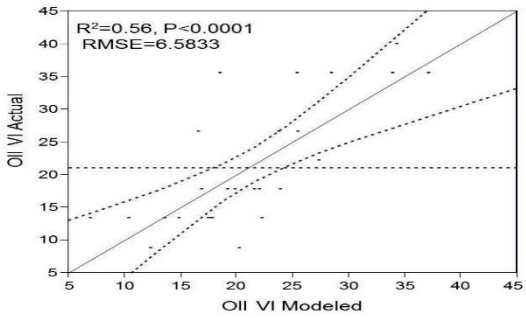

Figure 3. Modeling ozone damage visual assessment portion only (OII-VI) in Catalonia using remote sensing vegetation indices, ambient ozone concentrations averaged over the three years prior to the imagery acquisition

III. CONCLUSIONS

Good connections between the OII's individual components were observed in Catalonia's OII applications. Altitude, slope, aspect solar radiation, and topographic curvature are some of the GIS variables that are associated with plant water usage and availability; when combined with O3 ppb and OII components, this association also enhanced significantly. The scientific literature has long advocated for a more holistic and flux-based evaluation of ozone damage on forest health, particularly in areas similar to the Mediterranean [7]. This is a step in the right direction. We were able to estimate the overall health of the ecosystem by first identifying certain bioindicator species using image spectroscopy analysis techniques. Then, we used spectroscopy to estimate the physiology of all the individuals of these species for each valley. Although GIS cannot detect ozone flux into conifer needles via stomatal conductance directly, they can approximate the natural fluctuation over a landscape ([10]). This variability can explain a lot of the variation in ozone injury evaluations seen in the US and Europe ([8, 9]). When trying to link remote sensing with ozone damage using ambient ozone concentrations as a proxy, improved O3 uptake proxies are essential, particularly in climate regions similar to the Mediterranean, for the results to be significant. Lastly, after individual species are identified and a mix of biologically important variables is used to account for ozone flux and uptake, these methodologies should ideally be improved upon by O3-specific remote sensing vegetation indices.

REFERENCES

1. Jiménez-Muñoz J. C., Cristóbal J., Sobrino J. A., Sòria G., Ninyerola M., Pons X., 2009. Revision of the Single- Channel Algorithm for Land Surface Temperature Retrieval From Landsat Thermal-Infrared Data. IEEE Transactions on Geoscience and Remote Sensing, 47, 339-349

2. Landsat 7 Science Data Users Handbook, 2009. http://landsathandbook.gsfc. nasa.gov/handbook/handbook-t oc.html. Last accessed: Spetember,12, 2010
3. Noorollahi Y., Itoi R., Fujii H., Tanaka T., 2007. GIS model for geothermal resource exploration in Akita and Iwate prefectures, northern Japan. Computers & Geosciences 33, 1008-1021.
4. Qin Q., Zhang N., Nan P., Chai L., 2011. Geothermal area detection using Landsat ETM+ thermal infrared data and its mechanistic analysis - A case study in Tengchong, China. International Journal of Applied Earth Observation and Geoinformation 13, 552-559
5. Vaughan, R.G., Hook, S.J., Calvin, W.M., Taranik, J.V., 2005. Surface mineral mapping at Steamboat Springs, Nevada, USA, with multi-wavelength thermal infrared images. Remote Sensing of Environment 99, 140-158.
6. Yousefi H., Noorollahi Y., Eharaa S., Itoi R., Yousefi A., Fujimitsu Y., Nishijima J., Sasaki K., 2010. Developing the geothermal resources map of Iran. Geothermics. 39, 140-151.
7. Landsat 7 Science Data Users Handbook, 2009. http://landsathandbook.gsfc. nasa.gov/handbook/handbook-t oc.html. Last accessed: Spetember,12, 2010
8. Qiao Y., 2002. Primary investigation on applying infrared remote sensing technology to find groundwater. Spacecraft Recovery & Remote Sensing 23, 33-35
9. Sobrino, J.A., Jiménez-Muñoz, J.C., Paolini, L., 2004. Land surface temperature retrieval from Landsat TM5. Remote Sensing of Environment 90, 434-440.
10. T. A. Moore, "Coalbed methane: A review," International Journal of Coal Geology, Vol. 101, pp. 36-81, Nov 1, 2012.
11. R. Clarkson, "Production data analysis of unconventional gas wells: Review of theory and best practices," International Journal of Coal Geology, Vol. 109, pp. 101-146, Apr, 2013.
12. C. B. Ramos, and T. L. Davis, "3-D AVO analysis and modeling applied to fracture detection in coalbed methane reservoirs," Geophysics, Vol. 62, no. 6, pp. 1683-1695, Nov-Dec, 1997.